LA-UR-18-20675

Approved for public release; distribution is unlimited.

Title: Viscosity Control Experiment Feasibility Study

Author(s): Morris, Heidi E.
Bradley, Paul Andrew

Intended for: Distribution to colleagues at other institutions including AWE
Report

Issued: 2019-11-26 (rev.1)

Viscosity Control Experiment Feasibility Study (LA-UR-18-20675)

H. E. Morris* and P. A. Bradley

Los Alamos National Laboratory, Los Alamos, NM 87545

(Dated: January 31, 2018)

Abstract

Turbulent mix has been invoked to explain many results in Inertial Confinement Fusion (ICF) and High Energy Density (HED) physics, such as reduced yield in capsule implosions. Many ICF capsule implosions exhibit interfacial instabilities seeded by the drive shock, but it is not clear that fully developed turbulence results from this. Many simulations use turbulent mix models to help match simulation results to data, but this is not appropriate if turbulence is not present. It would be useful to have an experiment where turbulent mixing could be turned on or off by design. The use of high-Z dopants to modify viscosity and the resulting influence on turbulence is considered here. A complicating factor is that the plasma in some implosions can become strongly coupled, which makes the Spitzer expression for viscosity invalid. We first consider equations that cover a broad parameter space in temperature and density to address regimes for various experimental applications. Next, a previous shock-tube and other ICF experiments that investigate viscosity or use doping to examine the effects on yield are reviewed. How viscosity and dopants play a role in capsule yield depends on the region and process under consideration. Experiments and simulations have been performed to study the effects of viscosity on both the hot spot and the fuel/ablator mix. Increases in yield have been seen for some designs, but not all. We then discuss the effect of adding krypton dopant to the gas region of a typical OMEGA and a 2-shock NIF implosion to determine approximately the effect of adding dopant on the computed Reynolds number. Recommendations for a path forward for possible experiments using high-Z dopants to affect viscosity and turbulence are made.

* Email address: hmorris@lanl.gov

I. INTRODUCTION

Turbulent mix is ubiquitous in nature and has been invoked as one of the mechanisms responsible for preventing ignition at the National Ignition Facility (NIF) so far. The turbulent mix can be seeded by mounting features, such as fill tubes, glue spots or the "tent", or it can be seeded by irregularities in the surface finish of the capsule. In the latter case, Richtmyer-Meshkov (RM) and Rayleigh-Taylor (RT) instabilities can grow and mix material from the ablator or DT ice region into the hot fuel, limiting performance. These instabilities can arise on the interface of the pusher and the fuel and also between the low-density hotspot and surrounding higher-density fuel. As the capsule converges, the central fuel increases in density and can become more dense than the ablative pusher. While the outer surface of the pusher is stabilized against the Rayleigh-Taylor instability by ablation, the inner surface is not. Efforts have been made to reduce the Rayleigh-Taylor growth at the pusher/fuel interface by optimizing the density gradient, plasma viscosity, and mass diffusion. The Richtmyer-Meshkov instability arises when fluids of different density are impulsively accelerated by a shock wave. The fluids can mix chaotically creating bubbles where the low density fluid has penetrated the high-density fluid and spikes in density where the high density fluid has mixed into the low density fluid.

Analytic approximations give insight into the effect of dopants on viscosity and instabilities. In Section II the Spitzer viscosity is discussed and comparisons of the formulae for the RT growth rate with and without viscosity are made. Following Ref. [13], hydrogen is contaminated by a variable fraction of carbon and another high-Z dopant, krypton, to examine the effect on viscosity. In Section III past experiments and computational studies that examine the use of dopants are reviewed. The effect of dopants in reducing (or amplifying) these instabilities is of greatest interest, and recommendations for future experiments are made in Section IV. These will depend on the scale of the experiment and the plasma state that can be achieved.

II. PHYSICS CONSIDERATIONS

In this section equations that relate viscosity to instability growth and possible turbulence are considered. Low viscosity corresponds to high Reynolds number, and the timescale for the onset of turbulent growth is inversely proportional to the square root of the Reynolds number. Thus, we examine whether it is possible to increase the viscosity of a material by using dopants, and control turbulence.

The dynamic viscosity of a fully ionized plasma is reported in Ref. [6], and also Ref. [7]. The Rayleigh Taylor Instability (RTI) and its relevance for ICF was discussed in [7]. However, these authors [7] conclude that the effect of viscosity on RTI for ICF is negligible while compressibility is marginally important. In Ref. [7] it is concluded "It then turns out that viscosity can only reduce the growth of modes with wavelengths smaller than a fraction of a micron. It is instead ineffective on the modes with wavelengths of 15-60 μm, which are the most dangerous for the integrity of shells with in-flight thickness delta R about equal to 5-20 μm."

We start our evaluation with the Spitzer formula for viscosity which is also given in [8] as

$$\mu = 2.21 \times 10^{-15} \frac{T_i^{5/2} A^{1/2}}{Z^4 ln\Lambda} [\text{g cm}^{-1}\text{ s}^{-1}], \tag{1}$$

where T_i is the ion temperature in Kelvin, A is the atomic mass (amu), and Z is the atomic charge (as opposed to the mean ionization). The Coulomb logarithm is given by $ln\Lambda$. According to Eq. (1), viscosity has a strong inverse relationship with atomic charge. Thus, adding dopants of higher Z act to reduce the viscosity. As shown later, for a two component plasma, the viscosity can increase or decrease as a high-Z dopant is introduced into a hydrogen background plasma. The amount of increase or decrease and the change in viscosity with dopant fraction depends on the plasma temperature and density through the plasma coupling parameter.

The classical RTI growth rate, σ, is given in Ref. [7] (for fluids with no tangential velocity shear and neglecting surface tension) as

$$\sigma = \sigma_{RT} = (A_t a k)^{1/2}, \tag{2}$$

where $A_t = (\rho_2 - \rho_1)/(\rho_2 + \rho_1)$ is the Atwood number, k is the magnitude of the wavenumber, and a is the acceleration. For ICF implosions, $a > 10^{15}$ cm/s^2. However, an approximation of the growth rate that includes the effects of viscosity and compressibility is needed [11], which is given by:

$$\sigma = (A_t a k)^{1/2}[(1 + w)^{1/2} - w^{1/2}], \tag{3}$$

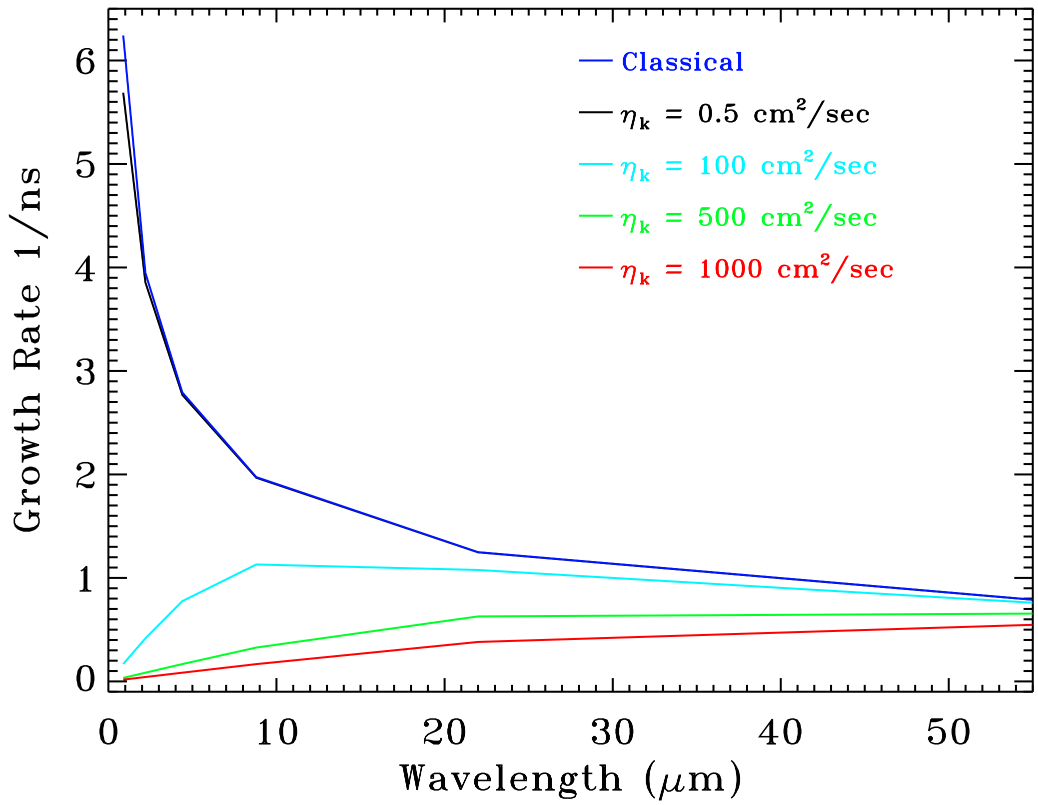

FIG. 1: RTI growth rate as a function of wavelength. The growth rate is reduced for all wavelengths as the viscosity increases. This effect is largest for shorter perturbation wavelengths.

where $w = \overline{\mu}_k^2 k^3 / A_t a$, $\overline{\mu}_k = (\mu_1 + \mu_2)/(\rho_1 + \rho_2)$ is the density averaged kinematic viscosity, and μ_1 and μ_2 are the dynamic viscosities of the two fluids. When w is small, the classical growth rate is recovered. However, when w is large the growth rate goes to zero. Using Eq. (1) for viscosity, it is possible to compute the RTI growth rate with Eq. (3) under ICF conditions. While it is difficult to apply Eq. (3) to plasmas where the density and temperature vary significantly in space, it is possible to estimate the effect of RTI at the interface between the hot plasma close to the ablation front and the dense shell. It may be of interest to estimate the effect of RTI between the inner fuel hot spot and the surrounding fuel. Based on Fig. 1 it appears that a kinematic viscosity of 0.5 cm^2/sec can only reduce the growth of modes with wavelengths smaller than a fraction of a micron. For the larger values of kinematic viscosity plotted here, the growth of modes less than 50 μm is reduced. However, this should be explored in a broader parameter space before making a general conclusion.

So far we have considered the Spitzer equation for viscosity, which applies for a single element, and the RT growth rate as a function of viscosity. However, experiments are composed of multiple materials that can mix and thus change the viscosity. We also wish to examine whether the use of multi-component, or doped, materials in experiments can control the viscosity.

We start with a one component plasma (OCP) model, the plasma is made up of positive particles with charge $Z_i e$ within a uniform non-responding negative background whose magnitude is such that the resulting net charge is zero. A pure hydrogen plasma is a one-component plasma and the plasma coupling parameter is expressed as Γ_0 when $Z_i = 1$.

$$\Gamma_0 = (e)^2/ak_BT. \tag{4}$$

The plasma frequency, (ω_p), for hydrogen is defined through

$$\omega_p^2 = 4\pi\rho(e)^2/m, \tag{5}$$

where m is the proton mass, and ρ is the number density of hydrogen atoms. For a fully ionized hydrogen plasma the electron and ion density are the same. For higher Z elements the electron density is Z_i times the atom density.

The two-component plasma is of immediate interest and is next considered in some detail. The ratio of the potential energy from Coulomb interactions to the thermal energy is called the plasma coupling parameter, Γ, and is given by

$$\Gamma = (Z_i e)^2/ak_BT, \tag{6}$$

where $(Z_i e)$ is the ionic charge which depends on the degree of ionization, a is the ionic sphere radius, and k_BT is the ionic temperature. Hot and diffuse plasmas are weakly coupled ($\Gamma << 1$), and the viscosity can be described by kinetic theory. Above the weakly coupled regime ($\Gamma > 0.5$), molecular dynamics (MD) simulations are often relied upon to model the viscosity.

For a mixture of two elements, such as dissociated CH, an effective coupling parameter, Γ_{eff} (see Fig. 2) is used in the place of Γ_0.

$$\Gamma_{eff} = \Gamma_0 \overline{Z}^{1/3}\overline{Z^{5/3}}, \tag{7}$$

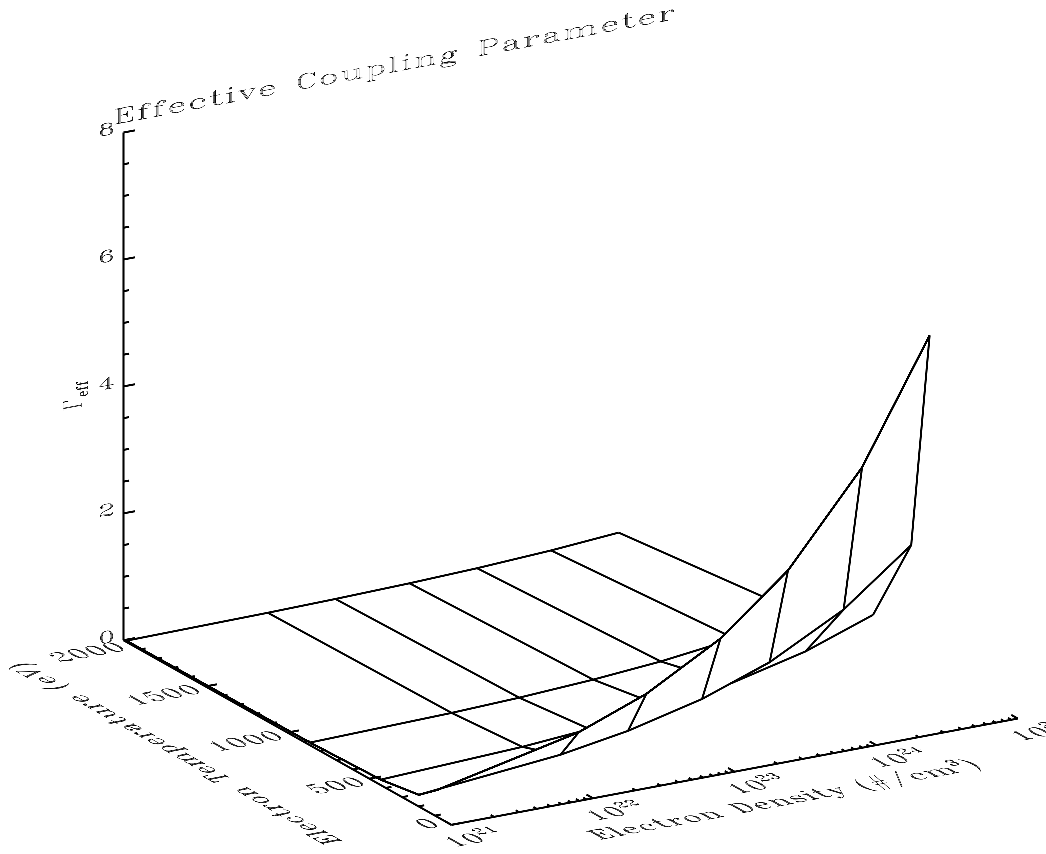

FIG. 2: The effective coupling parameter is shown for the values of electron number density and temperature considered here. A strongly coupled regime emerges for lower temperatures and higher electron densities.

where $\overline{Z} = x_1 Z_{i,1} + x_2 Z_{i,2}$ and $\overline{Z^{5/3}} = x_1 Z_{i,1}^{5/3} + x_2 Z_{i,2}^{5/3}$. Additionally, x_1 and x_2 are the fractions by number of the two components of the mixture. In Ref. [14] the viscosity is in units of $m_i \Omega_p \rho a^2$ so that it can be expressed in terms of the fractional, reduced viscosity η^*.

$$\eta = m_i \Omega_p \rho a^2 \eta^* \tag{8}$$

where ρ is the ion number density, $\Omega_p^2 = 4\pi\rho Z_i^2 e^2/m_i$, $m_i = Mm$, and M is the ionic mass. Thus, if hydrogen plasma units are used, the reduced viscosity must be multiplied by $\overline{Z}\sqrt{M}$.

The kinetic regime corresponds to plasma conditions where the coupling parameter is much less than one and the reduced viscosity then takes the form

$$\eta^* = 0.965 \frac{\sqrt{\pi}}{\sqrt{3}\Gamma^{5/2} \ln\Lambda}, \text{ where} \tag{9}$$

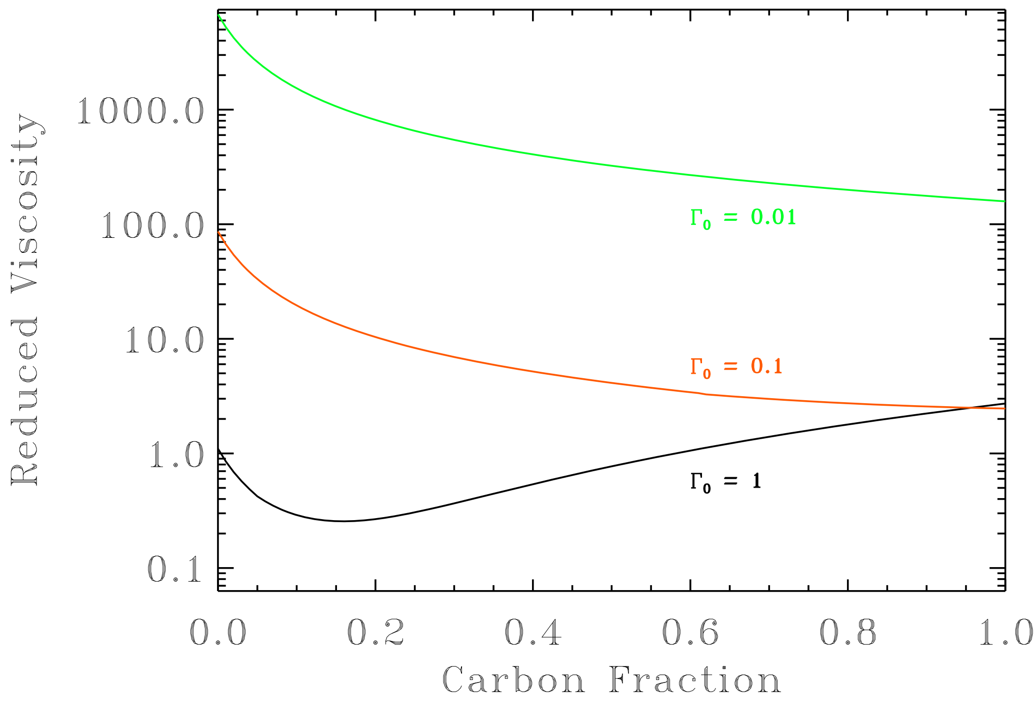

FIG. 3: Reduced viscosity as a function carbon fraction for a two-component plasma of carbon mixed with hydrogen.

$$\ln\Lambda = -\ln(\sqrt{3}\Gamma^{3/2}). \tag{10}$$

In order to extend the application to plasmas with Γ between 0.5 and 2, the extended Wallenborn-Baus (EWB) approximation was given in Ref. [13].

For $\Gamma_{eff} < 2$

$$\eta^* = 1.1\Gamma_{eff}^{-1.895} \tag{11}$$

For $2 < \Gamma_{eff} < 160$

$$\eta^* = \lambda I_1 + \frac{[1 + \lambda I_2(\lambda)]^2}{\lambda I_3(\lambda)}, \tag{12}$$

where $\lambda = \frac{4}{3}\pi(3\Gamma_{eff})^{3/2}$, $I_1 = (180\pi^{3/2}\Gamma_{eff})^{-1}$, $I_2 = (0.49 - 2.23\Gamma_{eff}^{-1/3})/(60\pi^2)$, and $I_3 = (2.41\Gamma_{eff}^{1/9})/(10\pi^{3/2})$. Since Γ_{eff} is given in terms of Γ_0, hydrogen plasma units are used and the reduced viscosity is multiplied by $\sqrt{M}Z$ in Figures 3 and 4.

In Figure 3 the carbon and hydrogen are treated as being fully ionized, as expected when $T \gtrsim 400$ eV. The green and orange curves show the reduced viscosity for two fixed values of the plasma coupling parameter for hydrogen, Γ_0=0.001 and 0.1, respectively. The viscosity for these two lower values of coupling parameter monotonically decrease as a function of the fraction of carbon that is added to the hydrogen plasma. However, when $\Gamma_0 = 1$, the viscosity initially decreases rapidly and then increases with carbon fraction > 0.1. This plot emphasizes the need to extend the analysis for a broad range of temperature and density to cover a larger experimental parameter space.

The situation for a heavier element, here krypton mixed into hydrogen, is shown in Figure 4. In contrast with the carbon results, the viscosity does not decrease monotonically with krypton fraction for any of the considered values of Γ_0. For $\Gamma_0 = 1$, the reduced viscosity can increase rather sharply after an initial drop at low krypton fraction. This happens to correspond to the case when krypton is added as a dopant to the DT central gas, where atomic fractions of 0.1 or less are used. However, for $\Gamma_0 = 0.01$ the viscosity starts high and drops dramatically, which would tend to inhibit and then suddenly allow turbulence as the krypton fraction is increased. Because these changes in viscosity with krypton fraction vary widely with the plasma state, a series of contour plots were created and could be improved for further consideration. They are not included in the discussion yet, since an average ionization of 34 ($Z_{Kr} = 36$) was used for krypton for all values of plasma temperature and density. A study with self-consistent average ionization is recommended, and would be a simple extension of the present work.

An estimation of the timescale required for turbulence has been given by [16]. This, and other authors define the outer-scale Reynolds number for turbulent flow as

$$Re = \delta u/\nu, \tag{13}$$

where u is the characteristic velocity, and δ is the outer length scale, which is the external-forcing energy containing scale and is on the order of the size of an experimental enclosure. Time is required to develop unsteady flows and a time criterion is defined as

$$t^* \geq (\delta/u)(100/C_D)^2 Re^{*-1/2}, \tag{14}$$

where $Re^* = 1.6 \times 10^5$ for their application. Above, C_D is the coefficient of the diffusion layer and is about 5 for laminar boundary layer flows and about $\sqrt{15}$ for homogeneous turbulence and steady parallel flows. However, the Reynolds number is treated as a variable that is a function of the plasma density and temperature through its inverse relationship

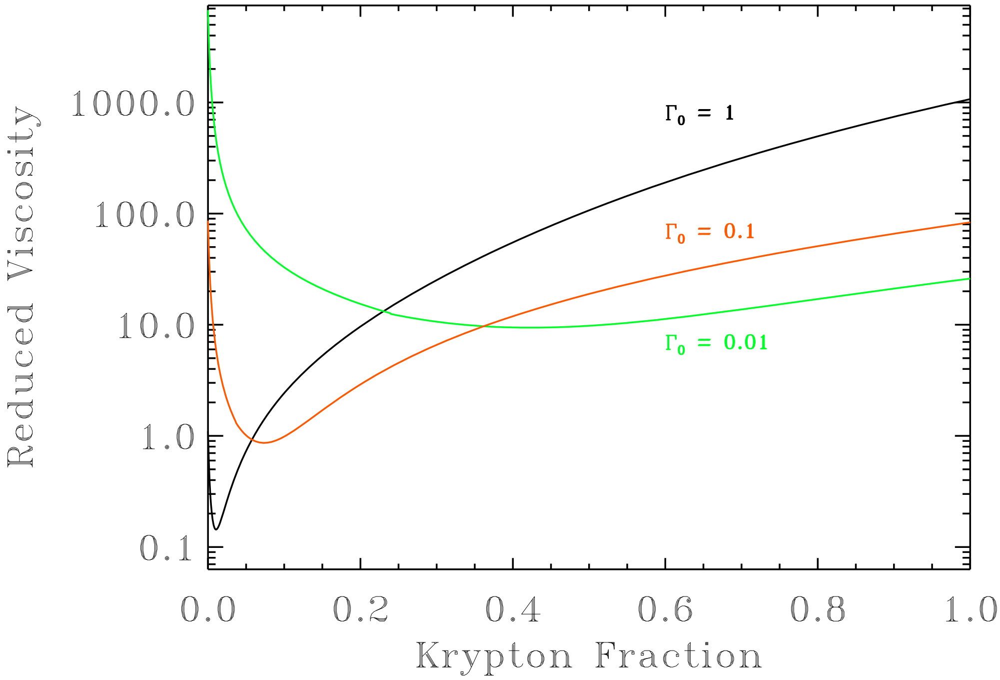

FIG. 4: Reduced viscosity as a function krypton fraction. This is a two-component plasma of krypton mixed with hydrogen.

with viscosity. Where the viscosity is low, the time required to achieve the turbulent state is also relatively low.

Deserving of further attention is Fig. 1 of Ref. [16], which is reproduced from an earlier work [17]. This figure shows the transition from turbulent to viscous states for phenomena of very different scales. In this spectral plot the energy contained in turbulence, or the inertial state, is characterized by a power-law fall off of -5/3. The energy in the viscous or dissipation state falls off more rapidly with increasing wavenumber. Transitions are characterized by the length scales λ_{LT} and λ_ν. Separation of the inertial (turbulent) and dissipation (viscous) ranges is described by λ_ν, and it can be approximated in terms of the Reynolds number by $\lambda_\nu = 50\delta Re^{-3/4}$. This parameter is of great interest for experiments transitioning to turbulence from viscous states and vice versa. Furthermore, the whole-system, or external forcing, and turbulent ranges have a boundary defined through $\lambda_{LT} = 5\delta Re^{-1/2}$.

III. EXPERIMENTAL FINDINGS

In this section experimental results that are relevant to the question of whether dopants can be used to change the viscosity and thus the hydrodynamics of an experiment are considered. For various experiments, dopants are often used to diagnose fuel conditions, including mix, and for ICF their effect on capsule performance is important.

The two-component plasma equations considered in the previous section were discussed by Ref. [8]. This work outlines a shock-tube experiment at Omega using a high density material (polyimide at 1.41 g/cm^3) adjacent to a low-density material (carbonized formaldehyde foam at 0.1 g/cm^3) with a sinusoidal interface. The system was shock heated for 1 ns using 10 beams with energy of 500 J/beam and an average power density of 5×10^{14} W/cm^2, and the deceleration and instability growth was radiographically imaged over several ns with a Ti backlighter producing 4.7-keV x-rays. The spatial scale of this experiment is about 1 mm, with perturbation length scales of a few microns. This author concludes that the dissipative effects of viscosity and mass diffusion are relevant for reducing the RT and RM growth rates for the small scales that were considered.

In these experiments [8], the perturbation growth was shown to evolve in a more random fashion as the number of modes was increased from one, two, and eight. It is shown that, for the conditions obtained in the experiment after the passage of the shock, the plasma coupling parameter is close to one, and because this is an uncertain regime, the kinematic viscosity is calculated using the single-material equations of both Clerouin and Braginskii. However, considering a variable mixture it is shown that the two-component plasma equations of Clerouin could be used to address mix. The kinematic viscosity is shown to vary by up to a factor of four depending on the polymide fraction. Ref. [8] discussed the importance of the diffusive transport of mass since it is comparible in magnitude with the viscous transport of momentum, and suggested the calculation of the Schmidt number times Reynolds number as being critical. Estimates of the Schmidt (Sc) number after the passage of the shock are 0.6, 1.0, and 1.5, where the largest number is for a material mixture. For this previous experiment, the product of the Reynolds and Schmidt number can be estimated using Eq. (13). Taking the outer scale length as 1 mm, and the characteristic velocity as the initial velocity of the contact discontinuity which is $8{\times}10^6$ cm/sec, and the reported kinematic viscosities of 0.04 to 0.2 cm^2/s, $Re \times Sc$ ranges from $4{\times}10^6$ to $2{\times}10^7$. The Schmidt number of 1.0 was used here. The time to transition to turbulence, through Eq. (14) ranges from 1.87 to 4.17 ns. Experimental radiographs at 13 ns showed advanced instability growth.

It may be possible to create an experiment similar to that presented in Ref. [8] where RTI growth occurs and viscosity is important using an interface of a high-Z material (or a material doped with a different high-Z material) and foam. If the high-Z mixes into the foam, the viscosity may initially be reduced and then increase as the high-Z material fraction becomes greater–for the right temperature and density conditions. Turbulence may then begin when the viscosity is low and then be quenched as more high-Z material is mixed in and the viscosity increases (See Figure 4). This experiment should be designed to perform near $\lambda_\nu = 50\delta Re^{-3/4}$, which defines the boundary between turbulent and viscous hydrodynamics [16]. Alternatively, a pair of shock-tube experiments could be performed where one is expected to become turbulent and the other is expected to have turbulence controlled through viscosity.

An experimental study of indirectly-driven high-growth RT and RM capsules [1] on NOVA [2] is of interest. Here, ablator dopants (1-3% Ge or Br) were used to give extra x-ray opacity to plastic capsules, providing preheat shielding of hard x-rays ($>$ 1keV) and reducing the entropy during the shell acceleration phase by about 20% for 1.3% dopant of Ge. The inner 3-μm of the shell was doped with 0.07% Ti as a spectral tracer and the 50-Atm DH fuel was doped with 0.05% Ar. These dopants diagnose the temperature and capsule nonuniformity at stagnation. These authors discuss the effect of adding dopants in terms of the dispersion relation for the RT growth rate, γ.

$$\gamma = \sqrt{[kg/(1+kL)]} - \beta k(dm/dt)/\rho \tag{15}$$

where L is the density scale length, the mass ablation rate is dm/dt, g is the acceleration or deceleration, k is the wavenumber of the seeding perturbation, β is an empirical constant, and ρ is the peak shell density. These authors [1] point out that adding a dopant to the ablator reduces preheat, which decreases the expansion of the shell and the mass ablation rate. The density of the shell, ρ, is therefore higher and because of several consequential factors the predicted linear growth of instabilities increases with increasing dopant levels. Nonetheless, these authors find an improvement in implosion performance with increasing amounts of Ge for the best surface finish plastic capsules. The average neutron yield increased monotonically from 0.25×10^9 to 1.2×10^9 as the percentage of Ge is increased from

0.0 to near 3%. In contrast the yield drops for roughened capsules with an increase in Ge, which suggests that the roughness seeds RTI growth.

Low levels of spectroscopic dopants are commonly used in the fuel region to diagnose fuel conditions. On Omega, thin shell glass capsules were used to confine a D-He^3 fuel [4] where Kr and Xe dopants were added to the gas. The neutron yield was higher than the neutron yield found on Nova, but it decreased with increasing amounts of dopant. For both Kr and Xe, the neutron yield dropped from 10^{11} to 10^{10} as the dopant pressure was increased from 0.01 to 1 atm. Slightly higher yields were measured for Kr than for Xe. Conversely, lower dopant pressure (Kr and Xe) resulted in higher yield. However, Ar did not appear to effect capsule yield for the pressure range of 0.001 to 1 atm [4]. It would help to compute Reynolds number and viscosity for these past experiments. The result for Argon was expected because of its low value of Z.

The importance of viscous dissipation in reducing RT instabilities has been addressed by Ref. [9]. In order to achieve ignition, a stable central region of temperature exceeding 10 keV is needed. Turbulence is believed to lead to less optimal conditions for hot spot formation and stability. For example, mix of cooler material into the hot region or hot material into the cooler, surrounding regions would be problematic. Turbulence around the hot spot could also alter the transport of energy that is intended to be directed radially toward the hot spot. However, it is shown that the hot spot is very viscous, with relatively low Reynolds number of 10-100, and the viscosity can damp out small velocity structures [9].

IV. CANDIDATE ICF EXPERIMENTS

As a further step to determine the feasibility of viscosity control experiments, we examined an OMEGA direct drive capsule implosion with a 1 ns square laser pulse [12] and a NIF indirect drive capsule with a 2 shock pulse [21]. We examined the plasma conditions during the implosion considering the addition of 0.001, 0.01, and 0.1 atomic fraction of Kr to the DT gas. We did not consider the self-consistent addition of the Kr to the gas EOS at this time, but this should be investigated later.

For the OMEGA experiment, we take the mix width of 10^{-3}cm and mix width growth of 10^6 cm/s from [12]. We then determine the viscosity about 100 ps before bang time when the DT gas conditions are 1.2×10^{22} cm^{-3} and 2170 eV and also at bang time, when

		Implosion Parameters					
		Early			Peak Burn		
		n_e [cm^{-3}]	ν [cm^2/sec]	R_e	n_e [cm^{-3}]	ν [cm^2/sec]	R_e
Omega	0% Kr	1.2×10^{22}	0.39	2560	4.2×10^{22}	0.78	1280
	10% Kr	4.2×10^{22}	0.86	1200	1.7×10^{23}	3.6	275
NIF	0% Kr	6.0×10^{22}	0.05	2×10^4	3.6×10^{23}	0.2	5000
	10% Kr	2.0×10^{23}	0.1	1×10^4	1.33×10^{24}	3.9	250

TABLE I: Typical parameters for fusion experiments

conditions are 4.2×10^{22} cm^{-3} and 3500 eV. We estimate that the ionization state of the krypton is about 25 for 2170 eV and 30 for 3500 eV. Table 1 shows the resultant electron density when the krypton is added, along with the viscosity and Reynolds number. The nominal implosion with pure DT has a low enough Reynolds number ($\sim$ 2500) for the flow to not be turbulent, but the addition of 0.01 or 0.1 atom fraction of krypton will drop the Reynolds number to 1000 or less, which would not lead to turbulence.

For the NIF experiment, we again take the mix width of 10^{-3}cm and mix width growth of 10^6 cm/s. We then determine the viscosity about 150 ps before bang time when the DT gas conditions are 6×10^{22} cm^{-3} and 1100 eV and at bang time, when conditions are 3.6×10^{23} cm^{-3} and 3000 eV. The ionization state of the krypton is about 23 for 1100 eV and 27 for 3000 eV. Table 1 shows the resultant electron density when the krypton is added, along with the viscosity and Reynolds number. The nominal implosion with pure DT would be turbulent, but the addition of 0.01 or 0.1 atom fraction of krypton will drop the Reynolds number to 1000 or less, which would not lead to turbulence.

These scoping calculations suggest that an experiment can be designed for the NIF with a large enough change to the Reynolds number to turn turbulence on or off. More careful, self-consitent simulations will be needed, along with an analysis of the diagnostic signatures that would show the transition from turbulent to more laminar flow implosions.

V. CONCLUSIONS

We have examined the importance of viscosity for possible future ICF or shock-tube experiments. A self-consistent simulation study should be performed for various materials whereby the ionization is determined for many physical states. Ionization and EOS tables as a function of plasma temperature and density would be incorporated into simulations, which would advance our understanding beyond what is considered here. Additionally, radiative cooling would have an effect of transitioning the plasma to a higher coupling parameter, which changes the behavior of the viscosity as a function of high-Z dopant fraction. Radiative cooling would also be accounted for in simulations. This work should be re-examined in the context of recent results by Ref. [19] and Ref. [20] since these authors have updated the work of Ref. [13]. A reasonable path forward may be to create companion experiments for a shock tube facility where one experiment is expected to be turbulent and a change of materials to include a dopant is not turbulent. ICF experiments similar to those discussed in Section IV should also be considered, and a diagnostic signature of turbulence should be defined. Existing calculations of viscosity, diffusion, and turbulence such as those used in RAGE [22] will be investigated in the context of the experimental results.

Acknowledgments

This work was performed under the auspices of the U.S. Dept. of Energy by the Los Alamos National Security, LLC Los Alamos National Laboratory. N. M. Hoffman and S. H. Batha are thanked for helpful discussions.

[1] O. L. Landen, C. J. Keane, B. A. Hammel, M. D. Cable, J. Colvin, R. Cook, T. R. Dittrich, S. W. Haan, S. P. Hatchett, R. G. Hay, J. D. Kilkenny, R. A. Lerche, W. K. Levedahl, R. McEachern, T. J. Murphy, M. B. Nelson, L. Suter, and R. J. Wallace, Indirectly Driven, High Growth Rayleigh-Taylor Implosions on Nova, J. Quant. Spectrosc. Radiat. Transfer, **54**, No. 1/2, pp. 245-255 (1995).

[2] E. M. Campbell, Laser Part. Beams **9**, 209 (1991).

[3] C. J. Keane, G. W. Pollak, R. C. Cook, T. R. Dittrich, B. A. Hammel, O. L. Landen, S. H. Langer, W. K. Levedahl, D. H. Munro, H. A. Scott, and G. B. Zimmerman, X-Ray Spectroscopic Diagnostics of Mix in High Growth Factor Spherical Implosions, J. Quant. Spectrosc. Radiat. Transfer, **54**, No. 1/2, pp. 207-220 (1995).

[4] W. J. Garbett, S. James, G. A. Kyrala, D. C. Wilson, J. Benage, F. J. Wysocki, M. Gunderson, J. Frenje, R. Petrasso, V. Yu Glebov, and B. Yaakobi, Journal of Physics: Conference Series, **112** (2008).

[5] T. J. Awe, K. J. Peterson, E. P. Yu, R. D. McBride, D. B. Sinars, M. R. Gomez, C. A. Jennings, M. R. Martin, S. E. Rosenthal, D. G. Schroen, A. B. Sefkow, S. A. Slutz, K. Tomlinson, and R. A. Vesey, Experimental Demonstration of the Stabilizing Effect of Dielectric Coatings on Magnetically Accelerated Imploding Metallic Liners, Phys. Rev. Lett., **116** (2016).

[6] L. J. Spitzer, *Physics of Fully Ionized Plasmas*. 2nd edn. Wiley Interscience, New York. [29, 79, 366], (1962).

[7] S. Atzeni and J. Meyer-Ter-Vehn, *The Physics of Inertial Fusion: Beam Plasma Interaction, Hydrodynamics, Hot Dense Matter*. International Series of Monographs on Physics 125. Oxford University Press Inc., New York. (2004).

[8] H. F. Robey, Effects of Viscosity and Mass Diffusion in Hydrodynamically Unstable Plasma Flows, Physics of Plasmas, **11**, 4123 (2004).

[9] C. R. Weber, D. S. Clark, A. W. Cook, L. E. Busby, and H. F. Robey, Inhibition of Turbulence in Inertial-Confinement-Fusion Hot Spots by Viscous Dissipation, Phys. Rev. E, **89**, 053106 (2014).

[10] S. I. Braginskii, Transport Processes in a Plasma, Rev. Plasma Phys., **1**, 205 (1965).

[11] K. O. Mikaelian, Effect of Viscosity on Rayleigh-Taylor and Richtmyer-Meshkov Instabilities, Phys. Rev. E, **47**, 1, 375 (1993).

[12] P. A. Bradley, The Effect of Mix on Capsule Yields as a Function of Shell Thickness and Gas Fill, Physics of Plasmas, **21**, 062703 (2014).

[13] J. G. Clerouin, M. H. Cherfi, and G. Zerah, The Viscosity of Dense Plasma Mixtures, Europhysics Letters, **42** (1), pp. 37-42 (1998).

[14] B. Bernu and P. Vieillefosse, Transport Coefficients of the Classical One-Component Plasma, Phys. Rev. A, **18** No. 5, pp. 2345-2355 (1978).

[15] Y. Zhou, B. A. Remington, H. F. Robey, A. W. Cook, S. G. Glendinning, A. Dimits, A. C. Buckingham, G. B. Zimmerman, E. W. Burke, T. A. Peyser, W. Cabot, and D. Eliason, Physics of Plasmas, **10** 5, 1883 (2003).

[16] Y. Zhou, Unification and Extension of the Similarity Scaling Criteria and Mixing Transition for Studying Astrophysics Using High Energy Density Laboratory Experiments or Numerical

Simulations, Physics of Plasmas **14**, 082701 (2007).

[17] S. G. Saddoughi and S. V. Veeravalli, Local isotropy in turbulent boundary layers at high Reynolds number, J. Fluid Mech. **268**, 333 (1994).

[18] Hui Chen, T. Ma, R. Nora, M. A. Barrios, H. A. Scott, M. B. Schneider, L. Berzak Hopkins, D. T. Casey, B. A. Hammel, L. C. Jarrott, O. L. Landen, P. K. Patel, M. J. Rosenberg, and B. K. Spears, On krypton-doped capsule implosion experiments at the National Ignition Facility, Physics of Plasmas **24**, 072715 (2017).

[19] J. Daligault and K. Rasmussen, Determination of the shear viscosity of the one-component plasma, Physical Review E **90**, 033105 (2014).

[20] G. Kagan, S. Baalrud, and J. Daligault, Influence of coupling on thermal forces and dynamic friction in plasmas with multiple ion species, Physics of Plasmas **24**, 072705 (2017).

[21] S.F. Khan, S.A. MacLaren, J.D. Salmonson, T. Ma, G. A. Kyrala, J. E. Pino, J. R. Rygg, J. E. Field, R. Tommasini, J. E. Ralph, D. P. Turnbull, A. J. Mackinnon, K. L. Baker, L. R. Benedetti, D. K. Bradley, P. M. Celliers, E. L. Dewald, T. R. Dittrich, L. Berzak Hopkins, N. Izumi, M. L. Kervin, J. L. Kline, S. R. Nagel, A. Pak, and R. E. Tipton, Symmetry tuning of a near one-dimensional 2-shock platform for code validation at the National Ignition Facility, Physics of Plasmas **23**, 042708 (2016).

[22] B. M. Haines, E. L. Vold, K. Molvig, C. Aldrich, and R. Rauenzahn, The effects of plasma diffusion and viscosity on turbulent instability growth, Physics of Plasmas **21**, 092306 (2014).